The Canadian Mineralogist
Vol. 39, pp. 785-795 (2001)

TRIVALENT IODINE IN THE CRYSTAL STRUCTURE OF SCHWARTZEMBERGITE, $Pb^{2+}_5\ I^{3+}\ O_6\ H_2\ Cl_3$

MARK D. WELCH§

Department of Mineralogy, The Natural History Museum, Cromwell Road, London SW7 5BD, U.K.

FRANK C. HAWTHORNE AND MARK A. COOPER

Department of Geological Sciences, University of Manitoba, Winnipeg, Manitoba R3T 2N2, Canada

T. KURTIS KYSER

Department of Geological Sciences, Queen's University, Kingston, Ontario K7L 3N6, Canada

ABSTRACT

The crystal structure of schwartzembergite from the San Rafael mine, Sierra Gorda, Chile, tetragonal, *a* 3.977(1), *c* 12.566(4) Å, *I*4/*mmm*, has been refined to an *R* index of 1.8% based on 103 unique observed ($I > 5\sigma I$) reflections. Schwartzembergite is optically biaxial, but long-exposure precession photographs show no evidence of non-tetragonal symmetry. The tetragonal structure consists of interleaved PbO and Cl sheets stacked along the four-fold axis. The Pb and I sites are both coordinated by four O atoms arranged in a square to one side of the cation, with Pb–O = 2.407(3) Å and I–O = 2.15(1) Å. The Pb and I sites are only 0.54(4) Å apart, and hence cannot both be occupied at the local scale. The Pb site is also coordinated by four Cl atoms at a distance of 3.331(3) Å and arranged on the opposite side of the site to the O atoms; this very asymmetric coordination is characteristic of Pb^{2+} exhibiting stereoactive lone-pair behavior. Bond-valence summation around the I site gives a value of 2.92 *vu* (valence units), indicating the iodine to be trivalent (rather than pentavalent, as has been assumed in previous studies); this is the first recorded occurrence of trivalent I in a mineral. Single-crystal polarized infrared and ^{1}H MAS NMR spectroscopies indicate the presence of structural H. Chemical analysis by electron microprobe and H-line extraction (1.20 wt.% H_2O) gave the formula $Pb^{2+}_5\ I^{3+}\ O_6\ H_2\ Cl_3$. Electron diffraction showed numerous superlattice reflections, suggesting a *C*- or *I*-centered orthorhombic supercell with $a = 2a_s$, $b = 6b_s$, $c = c_s$ (*i.e.*, an 8×24 Å supercell), where the subscript *s* denotes the (pseudo-) tetragonal subcell. The observed substructure and local bond-valence requirements indicate that the ($I^{3+}O_4$) groups cannot polymerize, and that I^{3+} must occur on both sides of the oxygen layer in each (Pb,I)O sheet. These constraints result in five possible motifs for the superstructure; one of these sheets somewhat resembles the ordered sheet in nadorite, $Pb^{2+}Sb^{3+}O_2Cl$, suggesting that this may be the pattern of order in schwartzembergite.

Keywords: schwartzembergite, crystal structure, electron diffraction, infrared spectra, NMR spectra, trivalent iodine, hydrogen-line extraction, electron-microprobe analysis, superstructure.

SOMMAIRE

Nous avons affiné la structure de la schwartzembergite [tétragonal, *a* 3.977(1), *c* 12.566(4) Å, *I*4/*mmm*] provenant de la mine San Rafael, Sierra Gorda, au Chili, jusqu'à un résidu *R* de 1.8% en utilisant 103 réflexions uniques observées ($I > 5\sigma I$). La schwartzembergite est optiquement biaxe, mais les clichés de précession de longue durée d'exposition ne révèlent aucun écart à la symétrie tétragonale. La structure tétragonale est faite de feuillets PbO et Cl empilés en alternance le long de l'axe de rotation 4. Les sites Pb et I sont en coordinence avec quatre atomes d'oxygène disposés en carré d'un côté du cation, avec Pb–O = 2.407(3) Å et I–O = 2.15(1) Å. Les sites Pb et I sont à une distance de 0.54(4) Å seulement, de sorte que les deux ne pourraient être occupés à la fois localement. Le site Pb est aussi en coordinence avec quatre atomes de Cl à une distance de 3.331(3) Å et disposés de l'autre côté par rapport aux atomes d'oxygène. Cet agencement fortement dissymétrique est caractéristique du Pb^{2+} ayant une paire d'électrons isolés et stéréoactifs. Une somme des valences de liaison autour du site I mène à une valeur de 2.92 unités de valence, indication que l'iode est trivalent (et non pentavalent, comme on le croyait). C'est ainsi le premier exemple connu de la présence de l'iode trivalent dans le règne minéral. Des spectres polarisés dans l'infra-rouge obtenus sur cristaux uniques et de résonance magnétique nucléaire (spin à angle magique) de ^{1}H indiquent la présence de l'hydrogène dans la structure. Une analyse chimique avec une microsonde électronique, complémentée par extraction quantitative de l'hydrogène (1.20% H_2O par poids),

§ *E-mail addresses*: mdw@nhm.ac.uk

mène à la formule $Pb^{2+}_5 I^{3+} O_6 H_2 Cl_3$. La diffraction des électrons montre de nombreuses réflexions dues à une surstructure, ce qui pourrait indiquer une surmaille orthorhombique à *C* ou à *I* centré, avec $a = 2a_s$, $b = 6b_s$, $c = c_s$ (*i.e.*, une surmaille mesurant 8 × 24 Å), le symbole *s* s'appliquant à la sous-maille (pseudo-) tétragonale. La sous-structure observée et les exigeances locales des valences de liaison indiquent que les groupes ($I^{3+}O_4$) ne peuvent devenir polymérisés, et que les ions I^{3+} doivent être disposés des deux côtés de la couche d'atomes d'oxygène dans chaque feuillet (Pb,I)O. D'après ces contraintes, il existe cinq motifs possibles pour expliquer la surstructure; un de ces feuillets ressemble quelque peu au feuillet ordonné dans la nadorite, $Pb^{2+}Sb^{3+}O_2Cl$. Ce même schéma pourrait donc s'appliquer à la schwartzembergite.

(Traduit par la Rédaction)

Mots-clés: schwartzembergite, structure cristalline, diffraction d'électrons, spectre infra-rouge, spectre de résonance magnétique nucléaire, iode trivalent, ligne d'extraction de l'hydrogène, données de microsonde électronique, surstructure.

INTRODUCTION

Schwartzembergite is a lead iodine oxy-hydroxy-chloride first described from Mina Santa Ana, Caracoles, Sierra Gorda, Chile, in 1864 by Domeyko, who wrote the formula as $Pb(Cl,I)_2 \cdot 3PbO$. Mücke (1970) investigated schwartzembergite in more detail, and showed that it is tetragonal, *a* 5.614(2), *c* 12.549(2) Å, and gave the formula as $Pb^{2+}_6 (I^{5+}O_3) O_2 (OH)_2 Cl_4$. The symmetry, cell dimensions and composition indicate that schwartzembergite is a member of the family of layered Pb–oxychloride minerals (Welch *et al.* 1996). These structures consist of alternating litharge-like PbO layers and sheets of Cl atoms, with a wide variety of small highly charged cations replacing Pb in the "litharge" layers. As part of our ongoing work on this group (Cooper & Hawthorne 1994, Symes *et al.* 1994, Welch *et al.* 1996, 1998, 2000), we have characterized the structure of schwartzembergite and present the results here.

EXPERIMENTAL

The crystals used in this work are from the San Rafael mine, Sierra Gorda, Chile, and were obtained from the Natural History Museum (BM 86453) and the Royal Ontario Museum (M15136); everything except the initial precession photography was done on sample BM 86453. Schwartzembergite occurs as wedge-shaped crystals with a curved outer surface that consists of several rounded parts separated by radial valleys that spread out over the surface. The (100) surface is sub-tangential to the curved surface of the wedge, and the *a* axis is subparallel to the radial structure of the wedge. In transmitted cross-polarized light, the wedge-shaped crystals give off-centered biaxial interference-figures with large 2*V* values, and the extinction is very irregular. Thus schwartzembergite is not tetragonal, although the X-ray-diffraction data are completely in accord with tetragonal symmetry.

Single-crystal precession photographs taken with Zr-filtered Mo*K*α X-radiation indicate tetragonal symmetry, with cell dimensions $a \approx 3.97$, $c \approx 12.55$ Å and reflections compatible with the space group *I*4/*mmm*. Long-exposure zero-level photographs (57 h with polaroid film) show no sign of any additional reflections. Cell dimensions (Table 1) were determined by least-squares refinement of the setting angles for 25 intense reflections automatically centered on a Nicolet *R*3*m* four-circle diffractometer using graphite-monochromatized Mo*K*α X-radiation. Intensity data were collected according to the procedure of Hawthorne & Eby (1985); relevant information concerning data collection, reduction and refinement is given in Table 1. A psi-scan absorption correction, modeling the crystal as a thin plate with a minimum glancing angle of 11°, reduced *R* (azimuthal) from 22.4 to 2.0%. The data were corrected for Lorentz, polarization, absorption and background effects, averaged and reduced to structure factors; of the 106 unique reflections, 103 were classed as observed [$I > 5\sigma(I)$].

Electron-microprobe analysis

A crystal fragment of schwartzembergite BM 86453 was mounted in epoxy for chemical analysis. An initial semiquantitative survey of the energy-dispersion spectrum using an Hitachi S–2500 analytical scanning electron microscope indicated that the only detectable elements are Pb, Cl and I. A Cameca SX–50 was used for quantitative analysis, operating in wavelength-dispersion mode with an accelerating voltage of 20 kV and a beam current of 20 nA for a 1 μm beam spot, using PbO, RbI and NaCl as standards. Back-scatter and sec-

TABLE 1 MISCELLANEOUS INFORMATION FOR SCHWARTZEMBERGITE

a (Å)	3.977(1)	crystal size (mm)	0.015 x 0.17 x 0.19
c	12.566(4)	Rad/Mono	MoKα/Graphite
V (Å³)	198.8(2)	Total unique |F	106
Space Group	*I*4/*mmm*	No. of F_o	103
		R (observed)	1.8%
		wR (observed)	1.5%

Unit-cell contents: $Pb^{2+}_6 I^{3+}_2 O_8 H_2 Cl_3$

$R = \Sigma(|F_{o1} - F_{c1}|)/\Sigma F_o$

$wR = [\Sigma w(|F_{o1} - F_{c1}|)^2/\Sigma F_{o1}^2]^{1/2}$, $w = 1/(\sigma F)^2$

TABLE 2. CHEMICAL COMPOSITION (WT.%) AND UNIT FORMULA (*apfu*)* FOR SCHWARTZEMBERGITE

	obs.	ideal		
PbO**	81.13(68)	81.62	Pb^{2+}	4.86
I_2O_5**	11.20(23)	11.04		
Cl**	7.95(8)	7.78	I^{5+}	1.04
H_2O*	1.20(5)	1.32		
	101.48	101.8	O	6
O Cl	1.79	1.76		
Total	99.69	100.00	Cl	3.13
	Pb/I = 4.90			
	(Pb + I)/Cl = 1.95		H	1.86

* calculated on the basis of 6 O-atoms *apfu*;
** average of 24 spot electron-microprobe analyses;
* by H-extraction line

ondary-electron images did not reveal the presence of any inclusions or zoning. Analyses were collected over a large area of the crystal fragment, and reduced using the PAP routine of Pouchou & Pichoir (1985). The unit formula was calculated on the basis of Cl = 1 *apfu* (atoms per formula unit); results are given in Table 2.

Electron diffraction

A JEOL CX200 transmission electron microscope (TEM; 200 kV) equipped with an LaB_6 filament was used, operating as described in Welch *et al.* (1996). A small fragment (BM 86453) was removed from part of the large crystal from which the fragment used for the crystal-structure study was taken, powdered and sedimented from a suspension in dry alcohol onto a 3 mm holey-carbon Cu grid. It was not possible to get structure images of schwartzembergite because of the strong absorption of electrons by this mineral, and the resulting weak diffracted beams. A similar problem was encountered in the case of parkinsonite, a related lead oxychloride mineral (Welch *et al.* 1996); exposures of 60–90 s were sufficient to record weak superlattice reflections in parkinsonite.

Analysis for H_2O

The H_2O content was measured by hydrogen-line extraction according to the method of Koehler *et al.* (1991).

IR spectroscopy

A {100} tablet of schwartzembergite 0.55 mm thick was cut from a single crystal of specimen BM 86453. A microscope equipped with a mapping stage and attached to a Bruker IFS 66v FT–IR spectrometer was used to record absorption spectra with a beam size of 150 μm, a liquid–nitrogen-cooled MCT detector, a KBr beam splitter and a Globar source. The polarized absorption spectra were collected with the polarizer at angles of 0°, 45° and 90° to the {001} cleavage trace, and averaged over 512 scans with a spectral resolution of 4 cm^{-1}.

^1H MAS NMR spectroscopy

^1H MAS NMR spectroscopy was done at room temperature using a Chemagnetics CXP400 multinuclear spectrometer operated at a frequency of 399.9 MHz. The sample (0.3 g) was spun in a zirconia rotor driven by a dry-nitrogen gas-flow at a frequency of 10 kHz. A pulse width of 2.5 μs and 5 s delay were used. Proton chemical shifts are reported relative to tetramethylsilane (TMS).

Crystal Structure: Solution and Refinement

Scattering curves for neutral atoms and anomalous-dispersion corrections were used with the software SHELXTL; *R* indices are of the form given in Table 1 and are expressed as percentages.

The structure was solved by direct methods. The *E* statistics suggest that the structure is centrosymmetric, and the solution with the highest combined figure of merit in the space group *I*4/*mmm* showed the Pb position. The remaining atoms were located by successive cycles of refinement and difference-Fourier synthesis. In the difference-Fourier map, there was a strong peak ~0.6 Å from the Pb atom and a negative peak at the Pb-atom position. The subsidiary peak was assigned to I, and the occupancies of the Pb and I sites were considered as variable, subject to the constraint that the occupancies sum to unity. Full-matrix least-squares refinement of all variables, including anisotropic displacements on all atoms, resulted in convergence at an *R* index of 1.8%. Final atom positions and anisotropic-displacement factors are given in Table 3, selected interatomic distances and angles are given in Table 4, and observed and calculated structure factors may be obtained from The Depository of Unpublished Data, CISTI, National Research Council, Ottawa, Ontario

TABLE 3. FINAL ATOM PARAMETERS FOR SCHWARTZEMBERGITE

		x	*y*	*z*	* U_{11}	U_{33}	U_{eq}
Pb	4e	0	0	0.1421(4)	0.0024(1)	0.0022(1)	0.0023(1)
I	4e	0	0	0.185(3)	0.0011(1)	0.0031(10)	0.0018(3)
Cl	2b	0	0	1/2	0.0024(1)	0.0040(3)	0.0029(1)
O	4d	1/2	0	1/4	0.0031(2)	0.0032(5)	0.0031(2)

* $U_{22} = U_{11}$, $U_{23} = U_{13} = U_{12} = 0$ Fractional site-occupancies: Pb: 0.833, I: 0.167

TABLE 4. SELECTED INTERATOMIC DISTANCES (Å) AND ANGLES (°) IN SCHWARTZEMBERGITE

Pb–O	2.407(3)	x4	I–O	2.15(1)	x4
Pb–Cl	3.331(3)	x4	I–Cl	3.65(2)	x4
			O–I–O	81.8(6)	x4
Pb–I	0.54(4)		O–I–O	136(2)	x2

TABLE 5. BOND-VALENCE TABLE (IN *vu*: VALENCE UNITS) FOR SCHWARTZEMBERGITE

	Pb	Σ	I
O*	$0.458^{\times 4}\downarrow$	1.84	$0.699^{\times 4}\downarrow$
Cl**	$0.115^{\times 4}\downarrow^{\times 8}$	0.92	$0.030^{\times 4}\downarrow$
Σ	2.292		2.916

* bonds to O from Brown (1981);
** bonds to Cl from Brese & O'Keeffe (1991).

K1A 0S2, Canada. An empirical bond-valence table is shown as Table 5.

Results

Description of the average structure

There is one unique Pb position, with a square array of four O atoms to one side at a distance of 2.41 Å, and a square of four Cl atoms to the other side at a distance of 3.33 Å. There is one unique I position in an environment similar to that of Pb, with I–O = 2.15 Å and I–Cl = 3.65 Å. The environment of Pb^{2+} observed here is typical of a cation with a stereoactive lone-pair of electrons: the bond-valence requirements are more-or-less satisfied by short bonds to anions arranged on one side of the cation, allowing the stereoactive lone-pair of electrons to project out into the space on the opposite side of the cation. The Pb and I atoms are 0.54 Å apart, and only one of the two sites can be locally occupied. The environment of each cation is shown in Figure 1.

FIG. 1. The environments of the Pb and I sites in schwartzembergite; Pb site is a black circle, O atoms are highlighted circles, I atom is a cross-hatched circle.

The average structure of schwartzembergite is shown in Figure 2. A series of puckered ladder-like sheets extend parallel to (001) and are intercalated with layers of Cl atoms (Fig. 2a). Inspection of a sheet in the [001] direction (Fig. 2b) shows it to be a (puckered) 4^4 plane net with Pb and O occupying adjacent vertices, exactly as in the structure of tetragonal PbO. However, the attitude of sheets adjacent along [001] is different from that in tetragonal PbO; alternate sheets are shifted by *a*/2 in schwartzembergite relative to their position in tetragonal PbO. This displacement has the effect of providing coordination of the interlayer Cl by (Pb,I).

Infrared spectroscopy

The background-corrected infrared spectra (0°, 45° and 90°) of schwartzembergite in the OH-stretching region are shown in Figure 3. All three spectra have three overlapping absorptions at around 3150, 3420 and 3530 cm^{-1}.

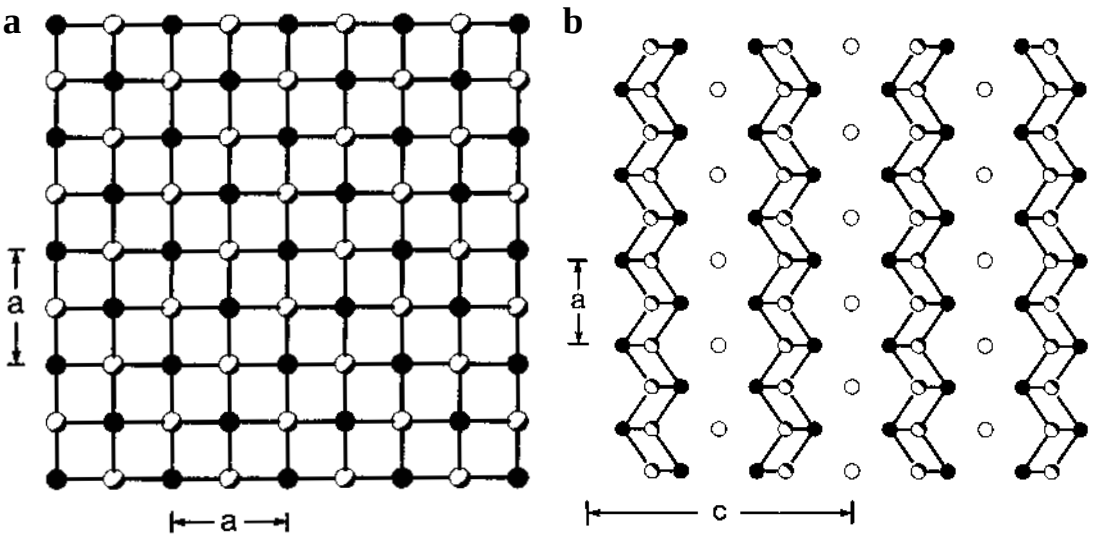

FIG. 2. The Pb–O sheet in schwartzembergite (a) viewed down [001]; (b) viewed down [100]; legend as in Figure 1. The Cl atoms are unfilled circles.

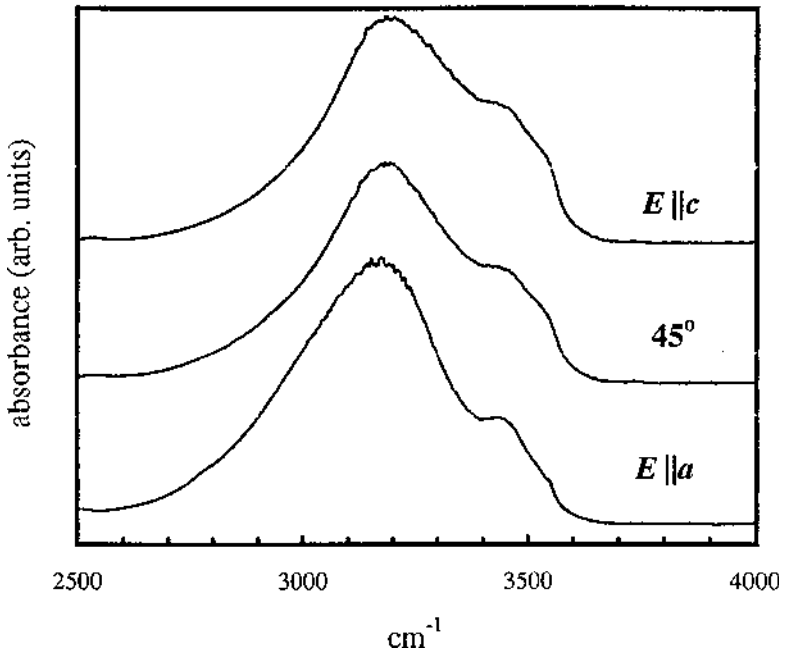

FIG. 3. The polarized infrared spectrum of schwartzembergite in the principal OH-stretching region.

^{1}H MAS NMR spectroscopy

The ^{1}H MAS NMR spectrum of schwartzembergite (Fig. 4) has two strong, narrow peaks at 1 and 4.5 ppm; there are two moderately intense, wider peaks at 6.7 and 8.6 ppm. The 1 ppm peak actually has two maxima at 0.8 and 1.3 ppm, and a sixth peak is present as a shoulder on the 1 ppm peak at 0.2 ppm. The peaks at 1 and 4.5 ppm are within the range of OH chemical shifts.

The chemical composition of schwartzembergite

A key result of the crystal-structure refinement is derived from a bond-valence analysis of the structure (Table 5): the incident bond-valence sum at I is 2.92 *vu*. This value indicates an I valence of 3^+ rather than 5^+ as has been previously assumed. Writing the formula of schwartzembergite as $Pb^{2+}_5\ I^{3+}\ O_6\ Cl_3$ leads to a charge deficit of 2^+ that can only be satisfied by incorporation of two H atoms into the structure to produce $Pb^{2+}_5\ I^{3+}\ O_6\ H_2\ Cl_3$. The postulated presence of H is in accord with the H-line extraction results, which gave a value of 1.20 wt.% H_2O. Table 2 shows that the chemical composition determined here is in accord with this value: the amount of H_2O required for electroneutrality is 1.32 wt.%, somewhat less than the value of 1.89 wt.% determined by Mücke (1970), and close to the value of 1.20 wt.% determined here.

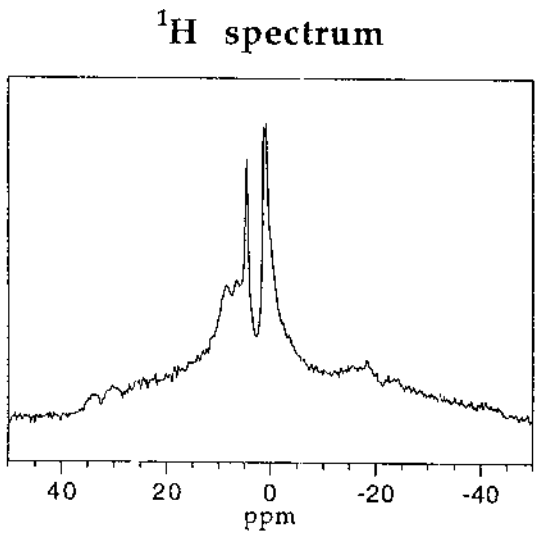

FIG. 4. The ^{1}H MAS NMR spectrum of schwartzembergite; peak positions are relative to tetramethylsilane (TMS).

The new formula for schwartzembergite gives a calculated density of 5.72 g cm^{-3}. This value is in exact agreement with that originally reported by Domeyko (1864, quoted by Mücke 1970): 5.7 g cm^{-3}, but is at variance with the measured values of 6.2 and 7.09 gcm^{-3} reported by Liebe (1867) and Mücke (1970), respectively.

Transmission electron microscopy

The electron-diffraction patterns of about ten crystallites of various sizes were collected. All patterns were obtained with the electron beam normal to the cleavage, due to the strong preferred orientation of cleavage flakes on the grid. This is advantageous because the strong {001} cleavage is parallel to the PbO layering of the schwartzembergite structure, and so is very suitable to test for any superstructure arising from Pb–I order. A representative *hk*0 electron-diffraction pattern of schwartzembergite using a 3-minute exposure is shown in Figure 5. Three kinds of reflections are present: A: relatively intense reflections due to the pseudotetragonal *I* subcell; B: weak but sharp reflections with a one-third $b^*_{subcell}$ periodicity; C: very weak reflections with a periodicity $(2n + 1)b^*_{subcell} / 6$ and showing faint streaking parallel to [010]*. B reflections were only recorded by exposures longer than one minute (Fig. 5a), and C reflections were only seen in 2- to 3-minute exposures (Fig. 5b). As we discuss below, the B and C reflections indicate a large superstructure. Some *hk*0 diffraction patterns show enhanced intensities for reflections at points corresponding to systematic absences for the *I*-centered subcell. The intensities of these reflections increase as a crystallite is tilted through a small angle (<3°), indicating that the violating reflections arise from spikes of diffracted intensity from the *hk*1 and *hk*1 layers. Such spikes are to be expected in view of the extreme thinness of the crystallites (cleavage flakes), for which it was possible to observe weak B and C reflections. Exposures of 2–3 minutes always showed these violating reflections (usually weak), indicating that *hk*1 and *hk*1 reflection spikes extend into the *hk*0 layer. Analogous observations were made by Welch *et al.* (1996) on the sheet oxychloride mineral parkinsonite.

For the same exposure times, the weak superlattice reflections observed by TEM of sahlinite (the As^{5+} analogue of kombatite) and symesite (Welch *et al.* 1996, 2000) have relative intensities (*i.e.*, relative to the intensities of sublattice reflections) that are comparable to the relative intensities of the B superlattice reflections (*i.e.*, relative to A reflections) of schwartzembergite. The superlattice reflections of kombatite and symesite were easily recorded by X-ray diffraction (Cooper & Hawthorne 1994, Welch *et al.* 2000). We would, therefore, have expected to record the B reflections (if not the very weak C reflections) of schwartzembergite by X-ray diffraction, and it is puzzling that they were not detected.

Discussion

Schwartzembergite superstructure

The B and C *hk*0 reflections define a reciprocal motif ($h + k$ even) that suggests a *C*- or *I*-centered orthorhombic supercell with $a = 2a_{sub}$ and $b = 6b_{sub}$ ($c = c_{sub}$). The corresponding sheet superstructure has twenty-four cation sites, which is compatible with the observed cation stoichiometry of schwartzembergite (*i.e.*, $Pb_{20}I_4$) and suggests that the superstructure arises from ordering of Pb^{2+} and I^{3+} within the (Pb,I)O sheet. The supercell is twelve times larger than the average *I*4/*mmm* subcell determined by X-ray diffraction. In passing, we note that the smallest sheet-superstructure possible for Pb_5I cation stoichiometry is a primitive motif ~4 × ~12 Å with six cation sites and chains of corner-linked IO_4 groups extending parallel to [100]. The *hk*0 diffraction patterns are not consistent with such a superstructure.

Here, we describe the possible geometrically distinct sheet-topologies arising from ordering of Pb^{2+} and I^{3+}, that lead to the 8 × 24 Å superstructure for Pb_5I cation stoichiometry ($Pb_{20}I_4$). Stacking of identical (Pb,I)O sheets having I^{3+} on one side of each oxygen layer does not lead to an *I*4/*mmm* average subcell, whereas stacking of sheets having equal numbers of I^{3+} on both sides of the oxygen layer does. The structurally related oxychloride sheet-mineral nadorite, $PbSbO_2Cl$ (Giuseppetti & Tadini 1973) has Sb^{3+} equally disposed on both sides of the oxygen layer. The possible geometrically distinct 24-cation-site sheet-topologies with an equal number of I^{3+} on each side of the oxygen layer and $Pb_{20}I_4$ cation stoichiometry are shown in Figure 6. All sheets, except sheet 2, have isolated IO_4 groups that form rows parallel to [100]; adjacent rows have I^{3+} on opposite sides of the oxygen layer. Sheets 1 and 2 have centered 8 × 24 Å motifs, whereas the other sheets have primitive 8 × 24 or 8 × 12 Å motifs. The primitive 8 × 24 Å and 8 × 12 Å variants of sheet 2 are omitted from Figure 6 for brevity. Sheet 2 has dimeric $[I_2O_6]$ groups.

In iodine oxide compounds with dimerized I^{3+} cations, such as $(IO)_2SO_4$ (Furuseth *et al.* 1974), I^{3+} forms two short bonds (~2.0 Å) as I–O–I linkages, and two much longer bonds (~2.4 Å) to the terminal oxygen atoms of the dimer. Other iodine oxide compounds having polymerized four-coordinated I^{3+} or I^{5+} (or both), such as I_2O_4, also have very asymmetric bonding arrangements around iodine, with two short and two long bonds (Fjellvåg & Kjekshus 1994). It seems, therefore, that where I^{3+} or I^{5+} or both are dimerized or form chains, the cation should be considerably off-center with respect to its four oxygen ligands. There is no evidence for such off-centering of I^{3+} in schwartzembergite, and so we can exclude topology 2 and its primitive variants as possibilities.

Figure 7 shows schematic *hk*0 diffraction patterns relevant to the interpretation of the observed electron-diffraction patterns of schwartzembergite. Firstly, we

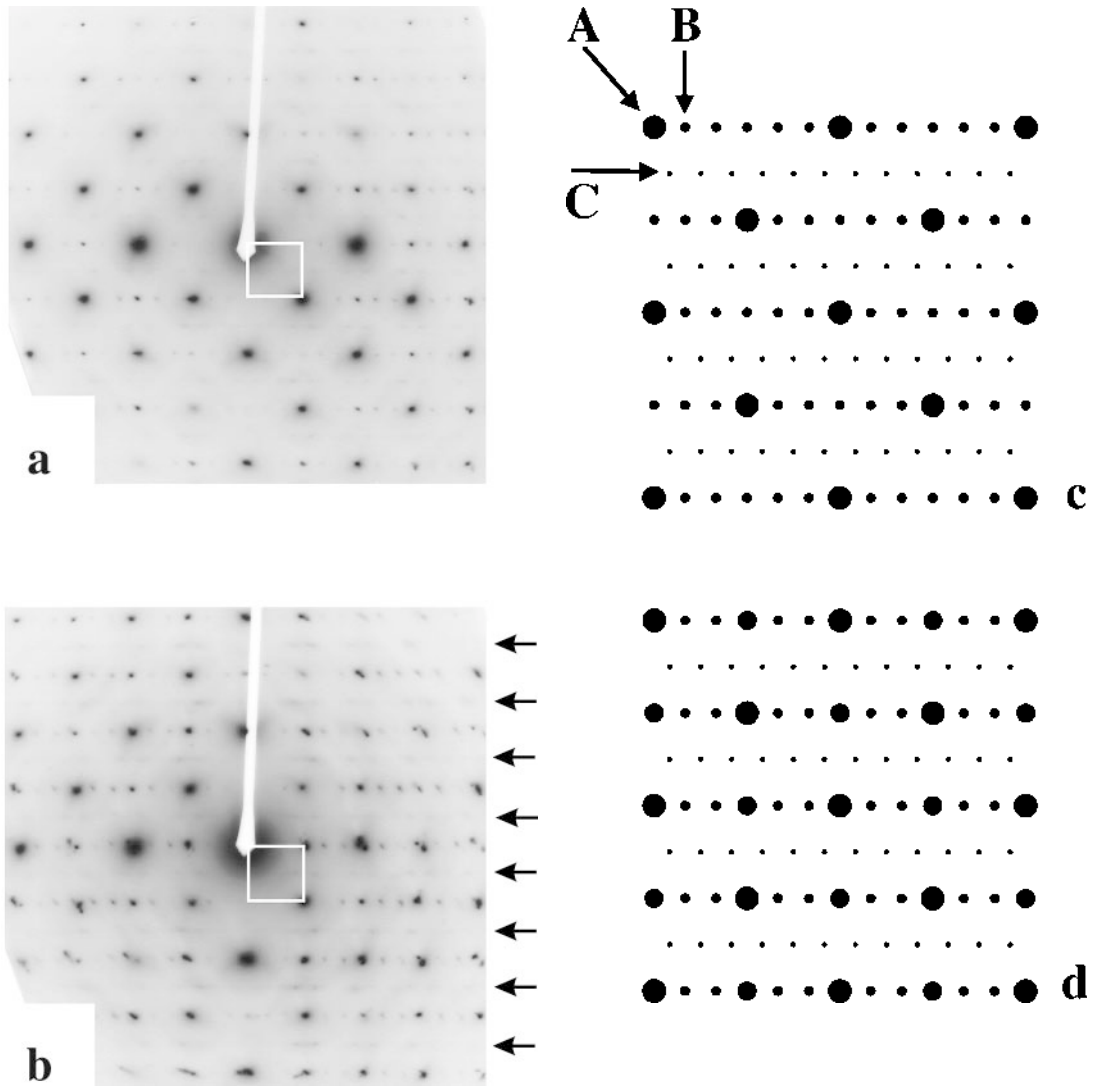

FIG. 5. *hk*0 electron-diffraction pattern of schwartzembergite: (a) Two-minute exposure showing relatively intense reflections due to the *I*4/*mmm* subcell. Rows of very weak B reflections parallel to [010] also are present. Some spots at forbidden ($h + k$ = odd) positions are diffraction spikes from sublattice reflections of the *hk*1 and *hk*1 layers. (b) Three-minute exposure of the same crystallite as in (a). The longer exposure time has allowed strong sublattice reflections from the *hk*1 and *hk*1 layers to be recorded. Rows of B reflections parallel to [010] are evident. Lines of weak spots from C reflections are indicated by arrows. Additional diffraction spots from a second crystallite that is slightly rotated relative to the main one also are present. This second crystallite is probably a piece of the main grain that became detached and rotated. Multi-crystalline patterns often confuse the interpretation of diffraction patterns of these easily cleaved, layered minerals. (c) Schematic diffraction pattern for 3(a). (d) Schematic diffraction pattern for 3(b).

see that a primitive 8 × 12 Å motif (sheet 4 in Fig. 6) is inappropriate. However, we make some further comments below on this motif with regard to interpreting the *b** streaking of C reflections. It is also evident from Figure 8 that primitive 8 × 24 Å motifs (sheets 3 and 5 in Fig. 6) also are ruled out. The closest qualitative agreement between theoretical and observed diffraction-patterns is for the centered 8 × 24 Å motif, *i.e.*, only sheet 1 in Figure 6.

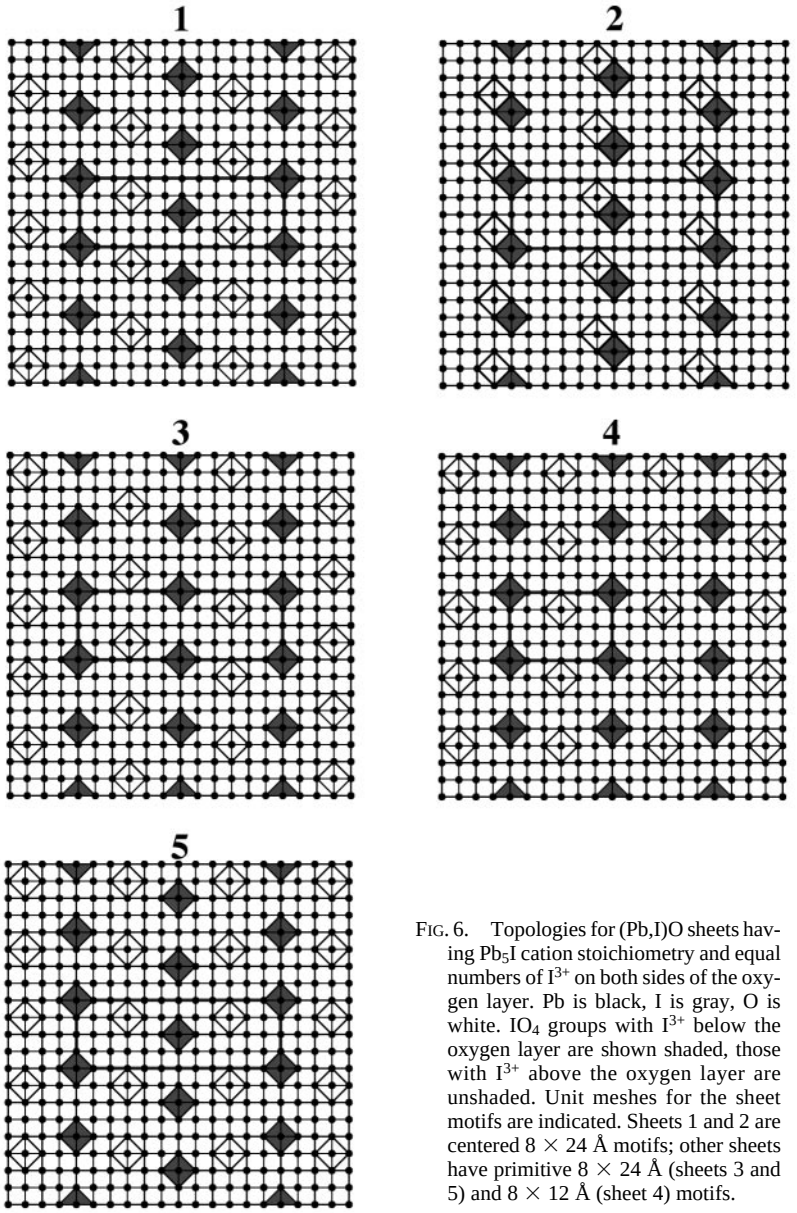

FIG. 6. Topologies for (Pb,I)O sheets having Pb_5I cation stoichiometry and equal numbers of I^{3+} on both sides of the oxygen layer. Pb is black, I is gray, O is white. IO_4 groups with I^{3+} below the oxygen layer are shown shaded, those with I^{3+} above the oxygen layer are unshaded. Unit meshes for the sheet motifs are indicated. Sheets 1 and 2 are centered 8 × 24 Å motifs; other sheets have primitive 8 × 24 Å (sheets 3 and 5) and 8 × 12 Å (sheet 4) motifs.

The observed streaking of C reflections parallel to *b** is consistent with some degree of intergrowth of centered 8 × 24 Å and primitive 8 × 12 Å motifs. Such an intergrowth would arise from stacking of 4 Å-wide (060) slabs of structure of Pb_5I cation stoichiometry (see above) along [010]. As the stacking involves the same structural element (*i.e.*, it is polytypic), we would anticipate that the energetics stabilizing centered 8 × 24 Å *versus* primitive 8 × 12 Å sheets are finely balanced. Note that an intergrowth of centered and primitive 8 × 24 Å motifs would result in streaking of all reflections parallel to *b**, which is not observed. However, given the undetermined superstructure and subtle nature of the "streaking", we cannot offer a definitive explanation of the streaking of the C reflections.

Insight into the probable sheet motif of schwartzembergite can be gained by looking at the structurally related sheet-oxychloride mineral nadorite, $Pb^{2+}Sb^{3+}O_2Cl$ (Giuseppetti & Tadini 1973). Nadorite has a PbO-based sheet consisting of alternate strips of Pb^{2+} and

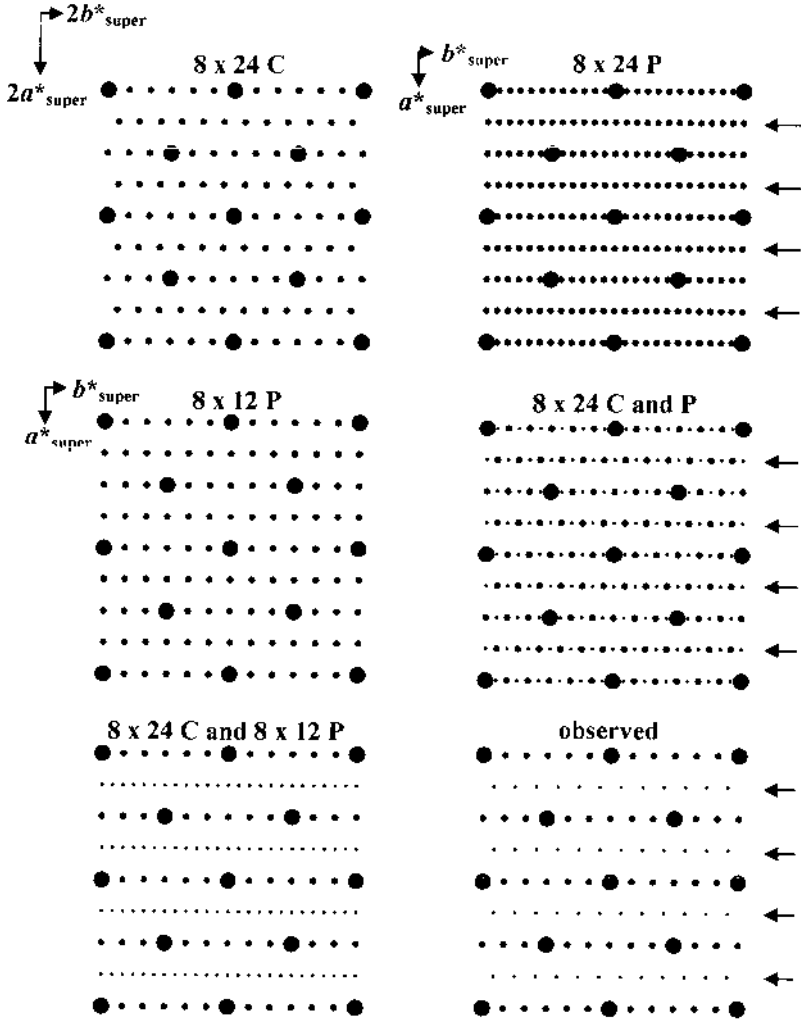

FIG. 7. Schematic *hk*0 electron-diffraction patterns for 8 × 24 Å and 8 × 12 Å sheets; the observed electron-diffraction pattern is at bottom right. Combinations of centered (C) and primitive (P) patterns are at middle right and lower left. Rows of *h* = odd reflections are arrowed. The combined electron-diffraction patterns correspond to coarse intergrowths of different sheets; unit-cell-scale stacking disorder due to irregular placement of chains leads to streaking of reflections parallel to [010]*.

Sb^{3+}. Each Sb^{3+} is coordinated to a square of four oxygen atoms and lies on one side of this square in the same way that I^{3+} does in schwartzembergite. Adjacent SbO_4 groups share edges, forming continuous strips of SbO_4 coordination polyhedra. Successive Sb^{3+} cations along each strip lie on opposite sides of the oxygen layer. If we now consider the four possible sheet motifs for schwartzembergite (sheets 1, 3, 4 and 5 in Fig. 6), we find that only sheet 1 has continuous strips of Pb^{2+}, as in nadorite. These Pb^{2+} strips alternate with strips having a cation composition Pb_2I (*i.e.*, $Pb_3 + Pb_2I = Pb_5I$). The Pb_2I strip of sheet 1 has pairs of Pb^{2+} between successive Sb^{3+}. The sheet topologies of nadorite and sheet 1 are compared in Figure 8. The structural similarity of the two topologies suggests that sheet 1 is likely to be the correct choice for schwartzembergite. Furthermore, sheet 1 is a 8 × 24 Å *C*-centered motif and so is consistent with the *hk*0 electron-diffraction patterns, which points to a 8 × 24 Å *C*- or *I*-centered supercell; sheets 3, 4, and 5 have primitive motifs. The streaking of C reflections parallel to [010] may arise from frequent faults at the unit-cell scale in the placement of succes-

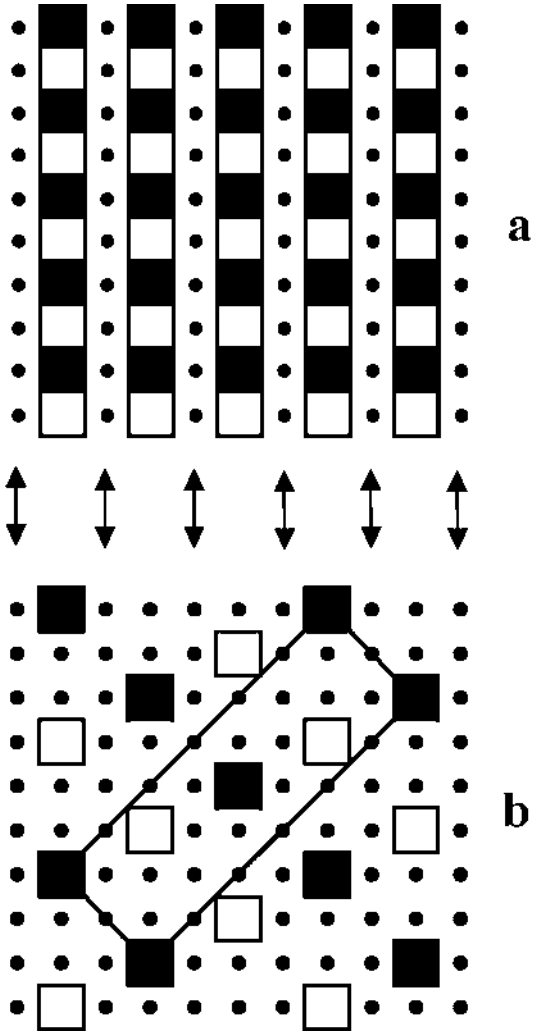

FIG. 8. Comparison of the topologies of the (Pb,M^{3+})O sheets of (a) nadorite $PbSbO_2Cl$, and (b) sheet 1 of schwartzembergite. M^{3+} groups are shown as squares, those with M^{3+} lying above the oxygen layer are white, those with M^{3+} below the oxygen layer are black. Pb^{2+} are black circles. The unit mesh of sheet topology 1 (see Fig. 6) is indicated. The continuous rows of Pb^{2+} in nadorite and sheet 1 are arrowed.

sive [100] rows of I^{3+} parallel to [010] during growth, leading to local sequences having motifs of sheets 3, 4, and 5.

Hydrogen in schwartzembergite

The crystallographic, analytical and spectroscopic data for schwartzembergite presented here all point to essential H in the structure. The formula we obtain is $Pb^{2+}{}_5\,I^{3+}\,O_6\,H_2\,Cl_3$. Both the infrared and ^1H NMR spectra indicate that there are several different H environments present in schwartzembergite. Furthermore, the 0° and 90° spectra are very similar, apart from slight increases in the relative intensities of the two weaker peaks at 3420 and 3530 cm^{-1}. The 45° spectrum is simply a combination of 0° and 90° spectra.

The average structure obtained from the X-ray structure refinement has symmetrically equivalent Pb–O and I–O bond-lengths; there is no evidence for some longer Pb–O and I–O bonds that could be associated with OH groups. The anisotropic-displacement factors for oxygen do not show any marked anisotropy or large variation, as might be expected if OH groups were present.

We were only able to record the diffraction pattern of the substructure by X-ray diffraction, despite extensive efforts to detect the superstructure recorded by electron diffraction. The lack of any X-ray evidence of superstructure indicates that the structural mechanism giving rise to the superstructure is very subtle. If the superstructure were involved in the ordered occurrence of OH, there would need to be major differences in the coordination of OH relative to that of O in the rest of the structure. This type of difference would produce changes in the average substructure that would have to involve the occupancies of the *Pb* sites plus the generation of new sites in order to maintain the observed Pb_5I stoichiometry. No such features are observed in the substructure refinement, indicating that H cannot be present as one or more ordered OH groups in the structure.

The infrared spectra are also instructive in this regard. In the principal OH-stretching region, a single OH group in an ordered crystal gives rise to a sharp absorption with a width in the range 2–50 cm^{-1}. In schwartzembergite, this region of the infrared contains a broad absorption with a half-width of ~600 cm^{-1}, with some additional shoulders. This absorption is somewhat reminiscent of what is observed in metamict titanite (Hawthorne *et al.* 1991), in which the H atoms are thought to have a large number of very different environments associated with a random-network metamict structure. By analogy, the broad absorptions in Figure 3 suggest that the H atoms in schwartzembergite adopt a large number of very different environments.

How is this latter deduction conformable with the ordered structure of schwartzembergite? Inspection of Figure 2 shows that the structure of schwartzembergite consists of layers of $[Pb^{2+}{}_5I^{3+}O_6]^+$ intercalated with layers of $[Cl_3]^{3-}$. It is the $[Cl_3]^{3-}$ layers that need the positive charge provided by the $(H_2)^{2+}$ in the structure, not the $[Pb^{2+}{}_5I^{3+}O_6]^+$ layers. Moreover, the O atoms of the $[Pb^{2+}{}_5I^{3+}O_6]^+$ layer lie along the center of this layer (Fig. 2), isolated from the $[Cl_3]^{3-}$ layer by the enveloping Pb^{2+} cations. It seems logical to conclude that the H atoms will reside in the $[Cl_3]^{3-}$ layer, rather than in the $[Pb^{2+}{}_5I^{3+}O_6]^+$ layer.

The details of the Cl environments in the superstructure are not available to us; we merely see an averaged planar sheet of Cl atoms. However, examination of the structure of kombatite (Cooper & Hawthorne 1994) shows that the Cl atoms of the intercalated sheets adopt very staggered positions on either side of the central plane. If this is the case in schwartzembergite, one expects numerous possible environments for H in this layer. Moreover, the H atoms are unlikely, for bond-valence reasons, to attach themselves strongly to a single Cl atom, raising the possibility of mobile, or "itinerant", H atoms within the $[Cl_3]^{3-}$ sheet.

Conclusions

1. Crystal-structure refinement of the 3.98 × 3.98 × 12.57 Å substructure of schwartzembergite indicates one-sided coordination of both Pb and I by a square of four O atoms, indicating stereoactive lone-pair behavior of Pb^{2+}.

2. Bond-valence analysis shows schwartzembergite to contain trivalent iodine; this it the first recorded occurrence of I^{3+} in a mineral.

3. Single-crystal polarized infrared and ^1H MAS NMR spectroscopies indicate the presence of structural H.

4. Electron-microprobe and H-line extraction analyses show the chemical formula of schwartzembergite to be $Pb^{2+}{}_5\ I^{3+}\ O_6\ H_2\ Cl_3$.

5. Electron diffraction shows the presence of a *C*- or *I*-centered supercell with $a = 2a_s$, $b = 6b_s$, $c = c_s$, where the subscript *s* denotes the substructure-cell dimensions.

6. A structure topology for the 8 × 24 (c = 12.5) Å superstructure is proposed.

Acknowledgements

We thank Lee Groat and an anonymous referee for their comments on the manuscript. This work was funded by Natural Sciences and Engineering Research Council of Canada Research, Major Equipment and Major Facilities Access Grants to FCH.

References

Brese, N.E. & O'Keeffe, M. (1991) Bond-valence parameters for solids. *Acta Crystallogr.* **B47**, 192-197.

Brown, I.D. (1981): The bond-valence method: an empirical approach to chemical structure and bonding. *In* Structure and Bonding in Crystals II (M. O'Keeffe & A. Navrotsky, eds.). Academic Press, New York, N.Y. (1-30).

Cooper, M. & Hawthorne, F.C. (1994): The crystal structure of kombatite, $Pb_{14}(VO_4)_2O_9Cl_4$, a complex heteropolyhedral-sheet mineral. *Am. Mineral.* **79**, 550-554.

Domeyko, I. (1864): Schwartzembergit. *Ann. Mines* V, 453.

Fjellvåg, H. & Kjekshus, A. (1994): The crystal structure of I_2O_4 and its relations to other iodine–oxygen containing compounds. *Acta Chem. Scand.* **A48**, 815-822.

Furuseth, S., Selte, K., Hope, H., Kjekshus, A. & Klewe, B. (1974): Iodine oxides. V. The crystal structure of $(IO)_2SO_4$. *Acta Chem. Scand.* **A28**, 71-76.

Giuseppetti, G. & Tadini, C. (1973): Riesame della struttura cristallina della nadorite: $PbSbO_2Cl$. *Per. Mineral.* **42**, 335-345.

Hawthorne, F.C. & Eby, R.K. (1985): Refinement of the structure of lindgrenite. *Neues Jahrb. Mineral., Monatsh.*, 234-240.

_____, Groat, L.A., Raudsepp, M., Ball, N.A., Kimata, M., Spike, F.D., Gaba, R.G., Halden, N.M., Lumpkin, G.R., Ewing, R.C., Greegor, R.B., Lytle, F.W., Ercit, T.S., Rossman, G.R., Wicks, F.J., Ramik, R.A., Sherriff, B.L., Fleet, M.E. & McCammon, C. (1991): Alpha-decay damage in natural titanites. *Am. Mineral.* **76**, 370-396.

Koehler, G.D., Chipley, D. & Kyser, T.K. (1991): Measurement of the hydrogen and oxygen isotopic compositions of concentrated chloride brines and brines from fluid inclusions in halite. *Chem. Geol.* **94**, 45-54.

Liebe, K. (1867): Näheres über das Jodblei aus Atacama. *Neues Jahrb. Mineral., Monatsh.*, 159.

Mücke, A. (1970): Schwartzembergit von der Mina Sta. Ana. *Neues Jahrb. Mineral., Monatsh.*, 467-472.

Pouchou, J.-L. & Pichoir, F. (1985): "PAP" $\phi(\rho Z)$ procedure for improved quantitative microanalysis. *Microbeam Anal.* **1985**, 104-106.

Symes, R.F., Cressey, G., Criddle, A.J., Stanley, C.J., Francis, J.G. & Jones, G.C. (1994): Parkinsonite, $(Pb,Mo,\square)_8O_8Cl_2$, a new mineral from Merehead Quarry, Somerset. *Mineral. Mag.* **58**, 59-68.

Welch, M.D., Cooper, M.A., Hawthorne, F.C. & Criddle, A.J. (2000): Symesite, $Pb_{10}(SO_4)O_7Cl_4(H_2O)$, a new PbO-related sheet mineral: description and crystal structure. *Am. Mineral.* **85**, 1526-1533.

_____, Criddle, A.J. & Symes, R.F. (1998): Mereheadite, $Pb_2O(OH)Cl$: a new litharge-related oxychloride from Merehead Quarry, Cranmore, Somerset. *Mineral. Mag.* **62**, 387-393.

_____, Schofield, P.F., Cressey, G. & Stanley, C.J. (1996): Cation ordering in lead – molybdenum – vanadium oxychlorides. *Am. Mineral.* **81**, 1350-1359.

Received June 14, 2000, revised manuscript accepted March 3, 2001.